

MemCast: Memory-Driven Time Series Forecasting with Experience-Conditioned Reasoning

Xiaoyu Tao¹ Mingyue Cheng¹ Ze Guo¹ Shuo Yu¹ Yaguo Liu¹ Qi Liu¹ Shijin Wang²

Abstract

Time series forecasting (TSF) plays a critical role in decision-making for many real-world applications. Recently, LLM-based forecasters have made promising advancements. Despite their effectiveness, existing methods often lack explicit experience accumulation and continual evolution. In this work, we propose MemCast, a learning-to-memory framework that reformulates TSF as an experience-conditioned reasoning task. Specifically, we learn experience from the training set and organize it into a hierarchical memory. This is achieved by summarizing prediction results into historical patterns, distilling inference trajectories into reasoning wisdom, and inducing extracted temporal features into general laws. Furthermore, during inference, we leverage historical patterns to guide the reasoning process and utilize reasoning wisdom to select better trajectories, while general laws serve as criteria for reflective iteration. Additionally, to enable continual evolution, we design a dynamic confidence adaptation strategy that updates the confidence of individual entries without leaking the test set distribution. Extensive experiments on multiple datasets demonstrate that MemCast consistently outperforms previous methods, validating the effectiveness of our approach. Our code is available at <https://github.com/Xiaoyu-Tao/MemCast-TS>.

1. Introduction

Time series forecasting plays a vital role in decision-making across a wide range of real-world scenarios, including energy scheduling (Qiu et al., 2024), financial trading (Feng et al., 2019), and healthcare monitoring (Huang et al., 2025b). More generally, TSF can be formulated as learning

¹State Key Laboratory of Cognitive Intelligence, University of Science and Technology of China, Hefei, China ²iFLYTEK Research, Hefei, China. Correspondence to: <>.

Preprint. February 4, 2026.

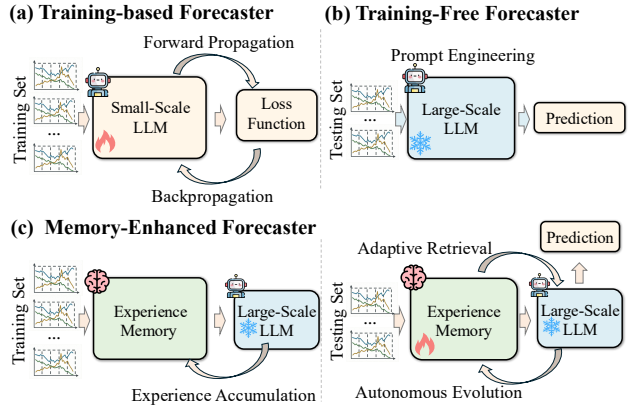


Figure 1. Comparison of training-based, training-free, and memory-enhanced LLM forecasting approaches.

a mapping from historical time series and associated contextual features, including dynamic features that vary over time (e.g., weather information) and static features that remain invariant across the forecasting horizon (e.g., location attributes), to future outcomes (Cheng et al., 2025a).

Building upon this formulation, TSF methods can be broadly categorized into several groups. Early statistical methods predict outcomes under predefined statistical assumptions (Hyndman & Khandakar, 2008). In contrast, data-driven deep learning approaches replace handcrafted statistical assumptions with automatic feature learning (Lin et al., 2025). Recently, LLM-based approaches leverage the capabilities of LLM for TSF (Huang et al., 2025a). These methods can be divided into two primary categories. As shown in Figure 1 (a), one line depends on backpropagation to update model weights, as represented by Time-LLM (Jin et al., 2024). As shown in Figure 1 (b), the other line adopts prompting strategies that directly harness the reasoning ability of large-scale LLMs, including LSTPrompt (Liu et al., 2024a) and TimeReasoner (Cheng et al., 2025b). These approaches offer advantages in capturing temporal dependencies with minimal data dependency.

Despite these advances, most existing approaches still exhibit two limitations. First, they generally treat forecasting instances as isolated reasoning, without explicitly converting historical outcomes across instances into reusable experi-

ence (Zhao et al., 2023). As a result, knowledge acquired from past predictions cannot be accumulated or transferred to benefit future forecasting tasks (Yang et al., 2025). Second, the absence of continual evolution limits the model’s potential for lifelong improvement, preventing it from adapting to newly observed forecasting instances (Chow et al., 2024). As illustrated in Figure 1(b), this observation motivates a memory-based learning approach that accumulates structured experience in an external memory while keeping the LLM parameters frozen, enabling adaptive retrieval and continual memory evolution during inference.

Based on the above analysis, we propose MemCast, a learning-to-memory framework that reformulates TSF as an experience-conditioned reasoning task. MemCast begins by extracting forecasting experience from the training set and organizing it into a hierarchical memory. Specifically, prediction outcomes are summarized into historical patterns, inference trajectories are distilled into reusable reasoning wisdom, and statistical features discovered from data are abstracted into general laws. During inference, historical patterns guide the reasoning process, reasoning wisdom supports the selection of effective reasoning trajectories, and general laws provide criteria for reflective iteration. To further support continual evolution without retraining, we introduce a dynamic confidence adaptation strategy that updates entry-level confidence while avoiding test set distribution leakage. Extensive experiments on multiple real-world datasets demonstrate that MemCast consistently outperforms existing methods, validating the effectiveness of learning experience and enabling memory-enhanced forecasting. We hope this work inspires further exploration of experience-driven learning for TSF.

2. Related Work

In this section, we review existing time series forecasting methods as well as recent LLM-based approaches.

2.1. Conventional Time Series Forecasting

Time series forecasting is extensively studied, with a wide range of methods proposed from different modeling perspectives. Early research primarily focuses on classical statistical approaches, such as ARIMA (Hyndman & Khandakar, 2008) and exponential smoothing (Winters, 1960), which model temporal dependencies based on predefined statistical assumptions. These methods can offer good interpretability, but their modeling capacity is inherently constrained by fixed assumptions and limited flexibility (Tire et al., 2024; Zhang et al., 2024). Subsequently, data-driven deep learning methods emerge as a dominant paradigm by replacing hand-crafted assumptions with automatic representation learning. Specifically, CNN-based models (Cheng et al., 2025c) emphasize local pattern extraction, RNN-based models (Wang

et al., 2019) capture temporal dependencies through recurrent mechanisms, GNN-based models (Feng et al., 2019) model relational structures among interconnected time series, and Transformer-based (Shi et al., 2025b) architectures are well-suited for modeling long-range interactions. In addition, MLP-based approaches (Zeng et al., 2023) demonstrate that simple architectures can achieve competitive performance with improved computational efficiency. Despite their success, such approaches typically require large-scale labeled data (Wang et al., 2025).

2.2. LLM-based Time Series Forecasting

Recently, LLM attracts growing interest for TSF, owing to its strong ability (Jiang et al., 2025). Existing LLM-based approaches typically leverage the knowledge encoded in pre-trained LLMs to alleviate data scarcity in TSF (Bian et al., 2024; Shi et al., 2025a). Depending on whether model parameters are updated, these methods can be broadly categorized into training-based and training-free approaches (Tang et al., 2025; Jia et al., 2024). Training-based methods (Jin et al., 2024; Luo et al., 2025) adapt LLMs to TSF through parameter-efficient fine-training or instruction training to better align them with forecasting objectives, with recent explorations also considering reinforcement learning. However, due to computational constraints, such approaches are usually applied to relatively small LLMs, which inherently limit their reasoning capacity (Liu et al., 2025a; Pan et al., 2024). In contrast, training-free methods (Xue & Salim, 2023; Liu et al., 2024a) increasingly adopt large-scale LLMs and exploit their powerful reasoning capabilities via prompt design and in-context learning, without requiring parameter updates. Despite their promise, existing LLM-based forecasting methods predominantly treat each forecasting instance in isolation (Yang et al., 2025).

3. Methodology

In this section, we first formalize the problem definition and then present the overview along with its key components.

3.1. Problem Definition

We consider a dataset $\mathcal{D} = \{(X_i, C_i, P_i)\}_{i=1}^N$ consisting of N time series instances. For each instance, $X \in \mathbb{R}^{T \times d}$ denotes the historical time series over T time steps with d dimensions, and C represents the associated contextual features aligned with the historical observations. Specifically, the contextual features include static features C^s and dynamic features $C^d = \{c_1^d, \dots, c_T^d\}$ aligned with the historical observations. The prediction target is the future time series $P \in \mathbb{R}^{H \times d}$ over a forecasting horizon H . Ultimately, the goal of time series forecasting is to learn a underlying mapping function $\mathcal{F} : (X, C^s, C^d) \rightarrow P$.

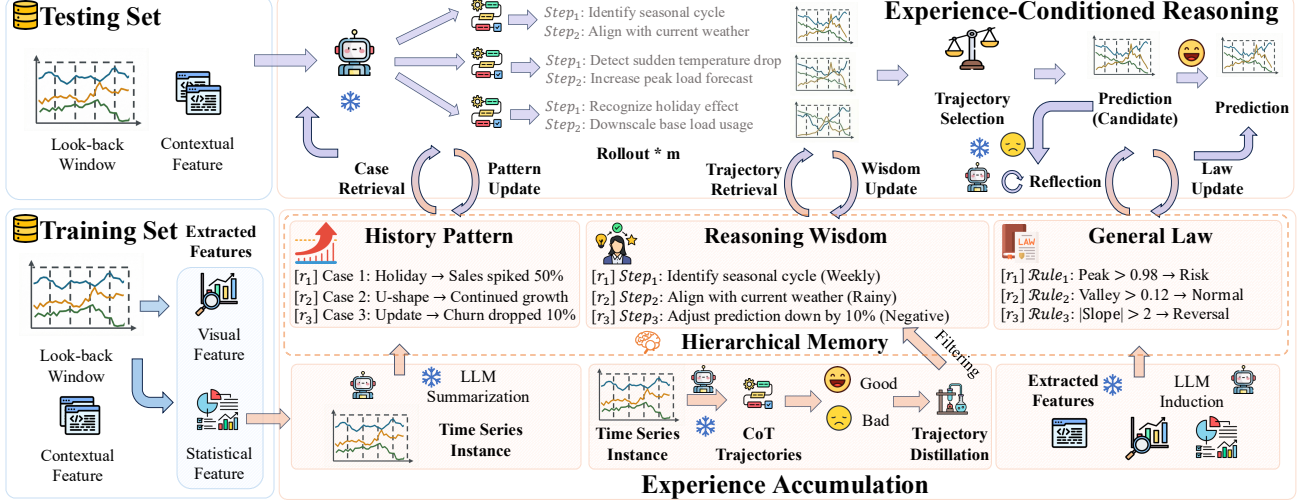


Figure 2. Overview of MemCast as an LLM-driven time series forecasting framework that constructs hierarchical memory from the training set via experience accumulation for experience-conditioned reasoning on the testing set.

3.2. Framework Overview

Figure 2 illustrates the overall framework of MemCast. In the experience accumulation phase, the framework learns from the prediction outcomes, inference trajectories, and extracted temporal features on the training set to build a hierarchical memory. In the experience-conditioned reasoning phase, MemCast utilizes the constructed hierarchical memory to support reasoning, trajectory exploration, and reflection, thereby enabling experience-conditioned reasoning without parameter retraining. Furthermore, a dynamic confidence adaptation strategy is employed to update the confidence of individual entries for continual memory evolution. The following subsections detail each component.

3.3. Experience Accumulation

Historical Pattern Abstraction. Instance-level historical patterns provide precise references for reasoning when encountering rare scenarios, particularly under distributional shifts (Cheng et al., 2025b). While such specific cases are valuable, directly feeding raw numerical values into LLMs is often ineffective for reasoning, as LLMs lack inherent sensitivity to numerical magnitudes and may fail to capture underlying temporal trends (Zhao et al., 2023). Building on the above analysis, we adopt a direct yet effective abstraction strategy that converts raw data into compact semantic summaries. Specifically, for each historical instance consisting of a lookback window $\mathbf{x} \in \mathbb{R}^L$ and a ground truth prediction window $\mathbf{y} \in \mathbb{R}^H$, we employ a summarization LLM \mathcal{S} to translate their numerical dynamics into descriptive natural language text. The final stored memory is structured as a paired summary $\mathcal{M}_{his} = (\mathbf{x}, \mathbf{m}_{out})$, defined as: $\mathbf{m}_{out} = \mathcal{S}(\mathbf{y})$, where \mathbf{m}_{out} encapsulates the trend evolution, volatility, and peak values, respectively.

Reasoning Wisdom Distillation. Reasoning trajectories serve as explicit logical bridges between raw observations and final predictions, making intermediate decision processes interpretable. However, existing approaches typically generate such trajectories at the instance level and discard them after a single inference, limiting their reuse across samples. A straightforward solution is to store and replay historical reasoning trajectories, but this is impractical due to the substantial redundancy and noise in raw reasoning outputs (Cao et al., 2025). To overcome these limitations, we adopt a simple yet effective strategy, termed reasoning wisdom distillation, to extract reusable reasoning experience from instance-level trajectories. Specifically, given a set of generated reasoning trajectories $\mathcal{C} = \{\mathbf{c}_i\}_{i=1}^N$ and their corresponding prediction errors $e_i = \mathcal{L}(\hat{\mathbf{y}}(\mathbf{c}_i), \mathbf{y}_i)$, we partition the trajectories into successful cases $\mathcal{C}_{pos} = \{\mathbf{c}_i \mid e_i < \tau\}$ and failed cases $\mathcal{C}_{neg} = \{\mathbf{c}_i \mid e_i \geq \tau\}$ based on a performance threshold τ . By analyzing these two groups separately, we distill success wisdom \mathcal{W}_{pos} and failure wisdom \mathcal{W}_{neg} , which together constitute the memory module $\mathcal{M}_{rea} = \{\mathcal{W}_{pos}, \mathcal{W}_{neg}\}$. We further implement a filtering to maintain a compact wisdom set, where similarity is computed as a combination of feature-level cosine similarity and raw space dynamic time warping (DTW). The composite similarity score $S(\mathbf{x}_q, \mathbf{x}_k)$ between a query sequence \mathbf{x}_q and a candidate sequence \mathbf{x}_k is defined as follows:

$$S(\mathbf{x}_q, \mathbf{x}_k) = \alpha S_{sem} + (1 - \alpha) S_{str}, \quad (1)$$

where $f(\cdot)$ denotes the feature embedding function and $\alpha \in [0, 1]$ is a weighting coefficient. The semantic similarity is computed as $S_{sem} = \text{CosSim}(f(\mathbf{x}_q), f(\mathbf{x}_k))$, while the structural proximity is measured by $S_{str} = \exp(-\text{DTW}(\mathbf{x}_q, \mathbf{x}_k)/\tau)$. Based on the combined score S , we replace redundant matches with $S > 0.95$, merge

overlapping cases with $0.8 < S \leq 0.95$ via LLM-driven fusion, and preserve novel patterns with $S \leq 0.8$.

General Law Induction. General laws aim to prevent the model from deviating from basic physical commonsense when adapting to new instances. While such laws could in principle be derived from instance-level analysis, the large scale of training data and the low information density of raw time series make this approach inefficient (Liu et al., 2025b). Building on this observation, we adopt a feature-level knowledge discovery strategy to induce general laws. Feature representations reduce redundancy, yet manual large-scale analysis remains impractical. We therefore leverage the general capabilities of LLMs as automated law inducers to analyze extracted temporal features and summarize general laws. Specifically, given a training dataset $\mathcal{D} = \{\mathbf{x}_i\}_{i=1}^N$ consisting of N raw time series samples, where $\mathbf{x}_i \in \mathbb{R}^T$. We design a toolset to automatically extract informative features from these samples. Moreover, we employ a textualization module that converts the numerical features of each sample into a textual description \mathbf{s}_i , enabling effective processing by LLMs. Based on a collection of these textualized representations, the LLM \mathcal{S} induces general laws that capture common principles: $\mathcal{M}_{gen} = \mathcal{S}(\{\mathbf{s}_1, \dots, \mathbf{s}_k\})$, where $\{\mathbf{s}_1, \dots, \mathbf{s}_k\}$ represents a cluster of representative samples derived from \mathcal{D} . Finally, the induced general laws \mathcal{M}_{gen} are used as self-reflection criteria during the inference.

3.4. Experience-Conditioned Reasoning

History-Enhanced Reasoning. LLMs primarily rely on parametric memory formed during pre-training. While this knowledge is rich, it is static and general-purpose, making it ill-suited for time series forecasting where data distributions shift over time (Liu et al., 2022). To bridge this gap, we propose experience-conditioned reasoning, which transitions the model from solely depending on internal parametric memory to leveraging external, dynamically accumulated experience, thereby enabling more effective utilization of training data. To ensure retrieval consistency across modules, we adopt the same similarity formulation defined in Eq. (1). This process identifies a subset of the top- k most relevant patterns, denoted as $\mathcal{C}_{sim} \subset \mathcal{M}_{his}$, serving as concrete analogical references. These retrieved cases are integrated to construct an augmented context. Consequently, the LLM’s inference process is transformed from a generic generation probability $P(Y|X)$ into an experience-conditioned probability $P(Y|X, \mathcal{C}_{sim})$.

Wisdom-Driven Trajectory Exploration. Despite the availability of training-derived experience, inference with LLMs remains inherently uncertain. Different reasoning trajectories may yield inconsistent predictions under similar inputs. Relying on a single reasoning pass, therefore,

risks amplifying stochastic errors and undermines reliability. We thus design an uncertainty-aware trajectory exploration strategy that jointly addresses uncertainty in LLM reasoning. For a query instance \mathbf{x} , we first compute a composite similarity score S , as defined in Eq. (1), for each candidate experience \mathcal{E}_j stored in the memory \mathcal{M}_{rea} . Based on these scores, we retrieve the top- k most relevant experiences to construct the augmented context set \mathcal{C}_{ret} . Then, the LLM samples M independent reasoning paths $\{(\mathcal{T}_m, \hat{\mathbf{y}}_m)\}_{m=1}^M$, where \mathcal{T}_m represents the generated chain-of-thought rationale and $\hat{\mathbf{y}}_m$ denotes the corresponding forecast values. To select the final output, we apply a scoring function $\phi(\cdot)$ that measures the semantic consistency of the trajectory \mathcal{T}_m against validated reasoning wisdom \mathcal{C}_{ret} . The candidate prediction $\hat{\mathbf{y}}$ corresponds to the candidate $\hat{\mathbf{y}}_{m^*}$ associated with the trajectory maximizing this reliability score: $\hat{\mathbf{y}} = \hat{\mathbf{y}}_{m^*}$, where $m^* = \arg \max_m \phi(\mathcal{T}_m)$.

Rule-Based Reflection. To mitigate the risk that predicted results may be inconsistent with real-world constraints, we design a rigorous rule-based reflection strategy. Specifically, after the model generates a candidate prediction $\hat{\mathbf{y}}$, we evaluate the predicted sequence against a pre-constructed set of domain-specific general laws $\mathcal{M}_{gen} = \{r_1, r_2, \dots, r_K\}$. These rules encapsulate essential constraints, such as non-negativity or range-bound continuity checks. Formally, if there exists a rule $r_k \in \mathcal{M}_{gen}$ such that the constraint $r_k(\hat{\mathbf{y}})$ is not satisfied, an immediate re-reasoning loop is triggered. Unlike simple rejection sampling, this loop feeds the specific violation details back into the LLM as a corrective prompt, forcing the model to revise its prediction. This iterative refinement continues until all constraints are met or a maximum retry limit is reached, ensuring that the final output Y is not only plausible but also compliant.

Dynamic Confidence Adaptation. Furthermore, we introduce a dynamic confidence adaptation strategy to leverage historical experience without test-data leakage. While memory accumulates experience during training, naively incorporating test-time outcomes can bias the model toward the test distribution. To this end, we decouple experience accumulation from utilization by assigning each frozen experience item \mathcal{E}_j a mutable confidence score r_j , initialized to zero. During inference, the generated prediction Y is evaluated against a moving average (MA) baseline. A prediction is considered successful only if it demonstrates superior reasoning ability, i.e., $\mathcal{L}_{LLM} < \mathcal{L}_{MA}$. In such cases, the confidence scores of the contributing experiences are increased to reinforce future selection, while unsuccessful attempts incur no updates. When $r_j > 0$, experience utilization considers both the confidence score and the retrieval similarity score S . This design updates only confidence weights rather than memory content, ensuring strict train–test separation and continual memory evolution.

4. Experiments

In this section, we first introduce the experimental settings and then present experimental results, ablation studies, and case analyses to evaluate the proposed framework.

4.1. Experimental Settings

Datasets. Table 1 provides detailed descriptions of the datasets used in our experiments, covering diverse forecasting scenarios and temporal scales with rich contextual features. Among them, NP, PJM, BE, FR, and DE from the electricity price forecasting (EPF) benchmark (Lago et al., 2021) provide short-horizon electricity price series from different regional power markets, together with corresponding contextual information such as load and generation forecasting. For long-term forecasting, ETTh and ETTm from the ETT benchmark (Zhou et al., 2021) mainly record transformer temperature and load measurements at different sampling frequencies. In addition, Windy Power (WP) and Sunny Power (SP) (iFLYTEK AI Challenge, 2025) contain renewable energy generation data accompanied by meteorological variables, while MOPEX (Makovoz & Marleau, 2005) collects hydrological streamflow with associated meteorological contextual features. These datasets exhibit diverse temporal dynamics and contextual dependencies, forming a comprehensive evaluation. Detailed dataset descriptions are provided in the Appendix A.1.

Baselines. We compare the MemCast against a diverse set of representative baselines, grouped into four categories for comprehensive evaluation. For statistical methods, we include ARIMA (Hyndman & Khandakar, 2008) and Prophet (Taylor & Letham, 2018), which model temporal patterns based on classical assumptions and trend decomposition. For deep learning-based approaches, we evaluate PatchTST (Nie et al., 2023), iTransformer (Liu et al., 2024b), TimeXer (Wang et al., 2024), ConvTimeNet (Cheng et al., 2025c), and DLinear (Zeng et al., 2023), which leverage advanced neural architectures such as Transformers, CNNs, and MLPs models to effectively capture temporal dependencies. In the LLM-based forecasting category, we consider LSTPrompt (Liu et al., 2024a), LLM-Time (Gruver et al., 2023), TimeReasoner, and Time-LLM (Jin et al., 2024), which adapt LLM to TSF through prompting, reasoning, and alignment mechanisms. Further implementation details are provided in the Appendix A.2.

Implementation Details. In this work, we use GPT-5 (Singh et al., 2025) as the reasoning engine for all LLM-based inference. By default, all experiments are conducted via the official API, with the temperature set to 0.6, top-p to 0.7, and the maximum number of generated tokens set to 16,384. Deep learning baselines are trained in PyTorch using the Adam optimizer on a single NVIDIA GeForce RTX

Table 1. Overview of diverse real-world datasets with rich contextual features. These benchmarks span multiple domains and temporal frequencies to ensure comprehensive evaluation.

Dataset	Domain	Length	Variables	Frequency
NP	Energy	14,496	3	1 hour
PJM	Energy	14,496	3	1 hour
BE	Energy	14,496	3	1 hour
FR	Energy	14,496	3	1 hour
DE	Energy	14,496	3	1 hour
ETTh	Electricity	12,240	7	1 hour
ETTm	Electricity	24,096	7	15 mins
WP	Energy	24,096	7	15 mins
SP	Energy	24,096	7	15 mins
MOPEX	Environment	12,240	6	1 day

4090D GPU, following official implementations and recommended hyperparameter configurations. For long-term forecasting tasks, both the look-back window and the prediction horizon are set to 96 time steps, while for short-term forecasting tasks, the look-back window is set to 168 and the prediction horizon to 24. Mean squared error (MSE) and mean absolute error (MAE) are adopted as evaluation metrics. For fair comparison, all models are evaluated on raw time series without normalization, so as to preserve the physical meaning of the original numerical values across all reported experimental settings.

4.2. Main Results

Table 2 summarizes the performance on diverse context-rich benchmarks. Overall, MemCast consistently achieves the best or second-best results across datasets, surpassing different baselines. Specifically, MemCast demonstrates consistently stronger performance than representative deep learning models across multiple datasets, with particularly noticeable improvements on highly volatile benchmarks such as NP and PJM. These results suggest that reasoning based on historical patterns may offer certain advantages in capturing irregular market dynamics, whereas approaches relying primarily on attention mechanisms may face limitations in such settings. Within the class of LLM-based forecasting methods, MemCast achieves lower prediction errors than Time-LLM on complex and noisy datasets such as BE. This observation indicates that, although fine-tuning-based approaches can adapt model behavior through parameter updates, their generalization ability may be challenged in high-noise scenarios. Furthermore, compared with TimeReasoner, MemCast attains more stable and consistently better performance across all benchmarks. This improvement is likely related to the explicit experience accumulation in MemCast, which allows historical forecasting experience to be reused across instances rather than being discarded after individual reasoning processes. Overall, these consistent gains empirically validate reformulating time series forecasting as experience-conditioned reasoning.

Table 2. Overall forecasting performance under short-term and long-term forecasting on various benchmark datasets. Lower values indicate better performance. The best results are highlighted in **bold**, and the second-best are underlined.

Model	NP		PJM		BE		FR		DE		ETTh		ETTm		WP		SP		MOPEX	
	MSE	MAE	MSE	MAE	MSE	MAE	MSE	MAE	MSE	MAE	MSE	MAE	MSE	MAE	MSE	MAE	MSE	MAE	MSE	MAE
ARIMA	78.944	5.722	181.141	9.944	6,813.559	20.889	3,072.651	16.878	414.126	14.568	8,992	2.314	4,456	1.725	2,504.541	32.558	120.801	6.595	7.703	1.680
Prophet	58.424	5.311	<u>63.342</u>	<u>6.102</u>	1,055.918	18.334	<u>999.577</u>	14.887	515.070	15.759	27.715	3.582	22.517	3.347	6,529.269	53.022	204.919	11.457	17.611	2.745
PatchTST	59.305	5.326	124,575	8.686	1,120.463	18.449	1,339.507	15.768	<u>290.971</u>	11.974	8,212	2.162	4,139	1.497	2,163.256	<u>31.822</u>	25.523	3.612	6,506	1.736
iTransformer	64.080	5.622	116.768	8.455	1,236.950	19.406	1,374.755	17.980	345.994	13.304	8,780	2.277	4,152	1.505	2,218.198	32.001	26.811	3.751	7.059	1.821
TimeXer	59.529	5.220	84.743	6.918	<u>887.125</u>	<u>14.463</u>	1,349.527	21.656	296.232	11.827	<u>7,913</u>	<u>2.137</u>	<u>4.026</u>	<u>1.463</u>	2,654.421	35.840	27.792	3.702	6,402	1.693
ConvTimeNet	55.857	5.111	108.312	7.935	1,146.507	18.191	1,175.164	15.096	327.377	12.727	9,101	2.356	4,346	1.593	2,128.109	32.496	27.381	3.802	7.102	1.831
DLinear	68.723	5.798	122.269	8.800	1,074.966	18.459	1,134.095	16.237	442.229	15.299	9,817	2.465	4,432	1.674	2,253.934	32.509	<u>23.720</u>	<u>3.506</u>	6,752	1.793
LSTPrompt	<u>53.062</u>	<u>4.933</u>	107,623	7.580	1,027.130	17.379	1,105.157	<u>14.419</u>	393.245	13.831	14,462	2.815	8,246	1.873	3,126.894	36.204	136.214	6.842	8.703	<u>1.692</u>
LLM-Time	92.740	6.446	158.170	9.350	1,283.180	20.078	780.831	12.877	1,282.570	17.935	27.387	3.316	5,398	1.811	4,438.044	38.913	131.182	5.617	6.729	1.497
TimeReasoner	70.514	5.447	56.471	5.168	1,028.621	12.509	1,212.133	9.628	629.794	6.088	10,357	2.431	1,574	3.625	2,500.350	32.284	17.599	1.847	5.465	1.442
Time-LLM	78.258	6.172	141.920	9.226	1,419.558	18.875	1,349.527	21.656	533.419	16.498	11,317	2.679	4,687	1.851	2,769.212	36.764	68.446	6.249	<u>6.274</u>	<u>1.692</u>
MemCast	36.871	3.567	30.238	3.575	756.308	12.534	756.981	12.142	210.445	9.195	6.551	1.968	3.999	1.441	2,170.456	31.715	22.998	1.876	6.193	1.525

Table 3. Ablation study on the different memory components: historical pattern, reasoning wisdom, and general law. The consistent performance degradation in “w/o” variants confirms the necessity of each module for accurate forecasting.

Method	NP		PJM		BE		FR		DE		ETTh		ETTm		WP		SP		MOPEX	
	MSE	MAE	MSE	MAE	MSE	MAE	MSE	MAE	MSE	MAE	MSE	MAE	MSE	MAE	MSE	MAE	MSE	MAE	MSE	MAE
w/o All	65.275	5.352	39.512	4.332	866.035	14.799	865.419	14.220	364.349	13.203	8,664	2.400	6,221	1.562	3079.615	36.355	25.255	2.043	15.111	1.978
w/o Law	46.463	<u>3.811</u>	<u>33.172</u>	<u>3.579</u>	<u>798.021</u>	<u>13.115</u>	821.493	13.116	<u>297.213</u>	<u>11.321</u>	<u>6.754</u>	<u>2.054</u>	<u>5.212</u>	<u>1.329</u>	<u>2712.801</u>	<u>35.937</u>	<u>23.488</u>	1.971	13.381	1.991
w/o Wisdom	55.545	5.334	33.301	3.731	858.120	14.165	826.714	13.816	314.471	12.319	8,215	2.326	5,592	1.716	2994.571	37.794	23.558	1.940	7.139	1.678
w/o Pattern	<u>45.594</u>	4.573	39.259	4.083	872.001	14.376	813.821	<u>13.444</u>	356.390	13.742	8,093	2.231	5,763	1.789	3656.032	39.969	30.340	2.084	10.978	1.916
Ours	36.871	3.567	30.238	3.575	756.308	12.534	756.981	12.142	282.801	10.903	6.551	1.968	3.999	1.441	2,170.456	31.715	22.998	1.876	6.193	1.525

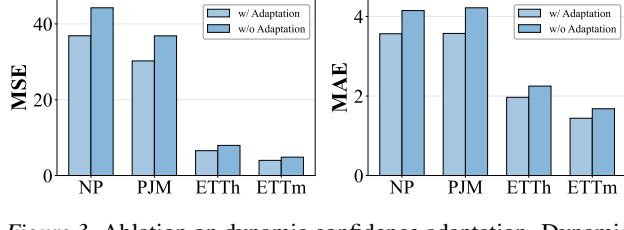


Figure 3. Ablation on dynamic confidence adaptation. Dynamic confidence adaptation leads to consistently lower errors compared with the variant without adaptation.

4.3. Ablation Studies

Ablation on Hierarchical Memory. Table 3 analyzes how different memory affect forecasting performance. Incorporating memory consistently yields substantial improvements over the memory-free baseline. We further decompose the experience memory into three components: general laws, which impose high-level distributional constraints; reasoning wisdom, which evaluates and verifies the logical consistency of the prediction process; and historical patterns, which capture instance-level evolutionary dynamics. While all contribute positively, distinct domain dependencies emerge. For instance, on PJM, removing reasoning wisdom causes a sharp drop, highlighting the need for logical validation in handling complex variations. In contrast, ETTh benefits more from general laws and patterns to capture periodic dynamics. Overall, the superior performance of the full model demonstrates its ability to integrate global constraints, logical verification, and instance cues for experience-conditioned forecasting.

Ablation on Dynamic Confidence Adaptation. Figure 3 presents the ablation results on dynamic confidence adaptation across multiple datasets. The variant with dynamic confidence adaptation consistently achieves lower MSE and MAE than the one without adaptation, with particularly noticeable improvements on the highly volatile NP and PJM datasets. This may indicate that dynamically updating confidence helps stabilize the reasoning process when facing rapidly changing conditions. On long-term benchmarks such as ETTh and ETTm, dynamic confidence adaptation also leads to consistent. These observations suggest that, beyond highly volatile scenarios, confidence updating remains beneficial for maintaining reliable performance over extended forecasting horizons. Overall, the results indicate that enabling the memory to continuously evolve during testing contributes to more stable performance.

4.4. Exploration Analysis

Exploration on Aggregation Strategy. Figure 4 illustrates the effectiveness of our uncertainty-aware trajectory exploration strategy. The experiment compares our approach against a baseline without refinement which relies on a single stochastic pass and a mean ensemble method that averages predictions across M sampled paths. While the mean ensemble yields marginal gains by smoothing out variance, it indiscriminately incorporates both high-quality rationales and inconsistent predictions thereby diluting accuracy. In contrast, our full model leverages the scoring function $\phi(\cdot)$ to measure the semantic consistency of each generated trajectory T_m against the retrieved reasoning wis-

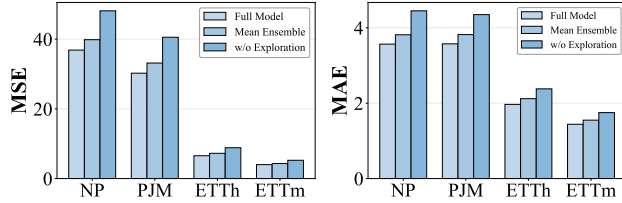


Figure 4. Exploration on aggregation strategies. The full model outperforms baselines, confirming that active selection via semantic consistency surpasses passive aggregation.

Table 4. Exploration on different LLM backbones. We evaluate the scalability of our framework across different LLMs.

Backbone	NP		PJM		ETTh	
	MSE	MAE	MSE	MAE	MSE	MAE
GPT-4o-mini	38.075	3.957	66.333	6.159	34.070	4.114
Gemini 2.5 Pro	61.822	5.149	41.077	4.121	6.726	2.030
DeepSeek-V3.1	41.707	3.539	145.995	5.021	27.066	2.633
Deepseek-R1	55.058	5.107	52.613	4.928	7.140	2.031
Ours	36.871	3.567	30.238	3.575	6.551	1.968

dom. By executing this generate-then-select protocol and specifically identifying the trajectory \mathcal{T}_{m^*} that maximizes the reliability score we effectively filter out stochastic noise. This suggests that active selection grounded in experience-conditioned consistency tends to outperform passive aggregation by better emphasizing reliable trajectories.

Exploration on LLM Backbone. Table 4 reports the scalability analysis of our framework instantiated with different LLM backbones. As shown in the table, we observe a clear positive correlation between the backbone’s reasoning capability and forecasting precision, with more advanced models consistently outperforming lightweight alternatives across all evaluated datasets. This performance trend validates that the proposed framework is able to effectively leverage the underlying reasoning capacity of the backbone, rather than relying on model-specific heuristics. Importantly, although our approach is model-agnostic, the default configuration achieves superior performance across all benchmarks, indicating a favorable balance between model capacity and reasoning effectiveness.

Exploration on Contextual Feature. Table 5 presents the ablation results on textual components, systematically evaluating their contribution to overall performance. The significant lead of our full model over the variant lacking all textual inputs strongly validates the critical value of textual inductive bias. Notably, sensitivity varies by domain: the highly volatile NP dataset degrades most without dynamic context, highlighting the need for instance-specific experience to capture rapid trend fluctuations. Conversely, PJM and ETTh rely more on static metadata as a robust reasoning anchor describing global properties. Ultimately,

Table 5. Exploration of contextual features. Integrating both static and dynamic features yields optimal performance.

Method	NP		PJM		ETTh	
	MSE	MAE	MSE	MAE	MSE	MAE
w/o All	41.133	3.403	42.315	4.469	8.041	2.249
w/o Dynamic	37.800	3.546	37.374	4.411	8.185	2.246
w/o Static	37.697	3.450	32.079	3.818	7.234	2.167
Ours	36.871	3.567	30.238	3.575	6.551	1.968

Table 6. Sensitivity analysis on the number of retrieved cases (k). Top- $k = 3$ consistently achieves the best performance.

Retrieval Number	NP		PJM		ETTh	
	MSE	MAE	MSE	MAE	MSE	MAE
Top- $k = 1$	37.347	3.657	37.120	3.902	7.808	2.207
Top- $k = 3$	36.871	3.567	30.238	3.575	6.551	1.968
Top- $k = 5$	43.095	3.979	40.643	4.092	6.691	2.155
Top- $k = 7$	46.155	4.134	45.221	3.865	7.362	2.207

the results confirm that static and dynamic contexts are mutually synergistic, essential for handling both invariant rules and complex time-varying dependencies.

4.5. Hyperparameter Sensitivity Analysis

Impact of Retrieval Volume. Table 6 presents a sensitivity analysis on the number of retrieved cases. Results indicate that a moderate number of cases yields the accurate performance, effectively balancing inductive bias against noise. When retrieval is minimal, the model struggles to abstract reliable commonalities, hindering generalization. Conversely, excessive retrieval degrades performance, as less relevant instances dilute the reasoning focus and introduce interference. Furthermore, we observe that while tasks requiring long-term dependency modeling benefit from slightly richer context, the moderate setting remains the most effective default for stable generalization.

Impact of Sampled Trajectory. As illustrated in Figure 6 (a), the forecasting error initially exhibits a significant downward trend as the number of sampled trajectories increases across all datasets. This suggests that generating multiple independent reasoning paths allows the model to explore a broader solution space and effectively mitigate individual hallucinations through consistency verification. However, performance gains tend to saturate or slightly degrade when the number of trajectories reaches a higher level (e.g., $m > 4$). This saturation indicates that while adequate sampling diversity is crucial for stability, an excessive number of paths may introduce lower-quality or redundant traces that dilute the final aggregation.

Impact of Sampling Strategy. As shown in Figure 6 (b), the results regarding sampling randomness exhibit a distinct U-shaped performance curve. A moderate temperature

Task: Forecast the next 96 hours of Oil Temperature (OT).

Context: The historical look-back window exhibits clear 24-hour seasonality with a consistent warming trend.

Covariate Alert: Future covariates indicate a temperature peak of 28°C (exceeding historical max) followed by a sharp drop to 16°C on the final day.

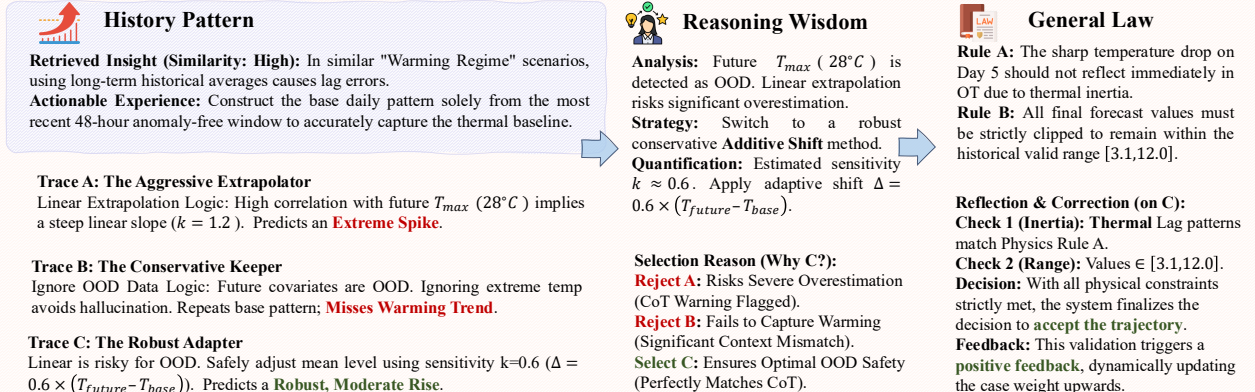


Figure 5. A detailed case study on the oil temperature (OT) forecasting task, illustrating experience-conditioned reasoning via constructed memory to effectively handle out-of-distribution thermal shifts.

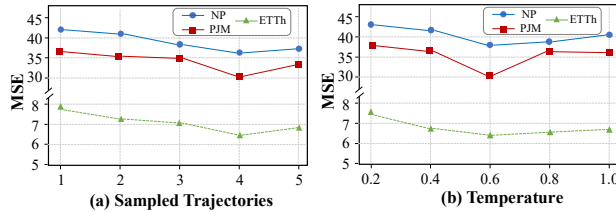


Figure 6. Hyperparameter sensitivity analysis regarding the number of sampled trajectories (a) and sampling temperature (b).

consistently yields the most favorable performance. At higher temperatures, the accuracy deteriorates, likely due to the injection of excessive randomness leading to unstable reasoning and hallucinations inconsistent with temporal constraints. Conversely, an extremely low temperature also results in suboptimal performance, suggesting that overly deterministic decoding limits the diversity of the model and its ability to adapt to complex, non-stationary patterns. Therefore, selecting a moderate temperature effectively balances the need for precise, rigorous reasoning with sufficient diversity to capture potential regime shifts.

4.6. Case Study

To intuitively demonstrate how MemCast mitigates reasoning hallucinations under distribution shifts, we analyze an oil temperature (OT) forecasting scenario where future covariates exhibit an anomalous out-of-distribution (OOD) peak of 28°C . Faced with this "Warming Regime," the history pattern memory first retrieves actionable experience to construct a baseline solely from the recent 48-hour window, thereby avoiding lag errors associated with long-term averages. Subsequently, the reasoning wisdom acts as a logical

filter, scrutinizing generated trajectories to reject both the aggressive linear extrapolation of Trajectory A ($k = 1.2$) and the overly conservative stagnation of Trajectory B. Instead, it selects the effective adapter (Trajectory C), which applies a moderate sensitivity ($k = 0.6$) to balance the covariate's influence with historical inertia. Finally, the prediction is validated by the general law, ensuring compliance with physical constraints such as the valid range of [3.1, 12.0]. This process highlights MemCast's ability to actively reason through physical constraints rather than blindly following misleading OOD signals in challenging real-world scenarios.

5. Conclusion

In this work, we presented MemCast, a learning-to-memory framework that reformulates time series forecasting as an experience-conditioned reasoning problem. By explicitly accumulating forecasting experience from the training set, MemCast constructs a hierarchical memory composed of historical patterns, reasoning wisdom, and general laws, enabling the model to move beyond instance-level reasoning. During inference, these complementary memory components collaboratively guide reasoning, trajectory selection, and reflective correction, while a dynamic confidence adaptation strategy supports continual evolution without introducing test-data leakage. Extensive experiments across diverse datasets demonstrate that MemCast consistently outperforms existing approaches, highlighting the effectiveness of explicit experience abstraction and controlled memory utilization for accurate time series forecasting. We believe that MemCast offers a promising step toward experience-aware forecasting with continual evolution.

Impact Statement

This work advances time series forecasting through MemCast, an experience-conditioned reasoning framework that enhances interpretability and reliability in critical domains such as energy and healthcare. By integrating general laws to enforce physical constraints and employing dynamic confidence adaptation for autonomous evolution, our approach effectively mitigates generative hallucinations and adapts to non-stationary environments.

References

Bian, Y., Ju, X., Li, J., Xu, Z., Cheng, D., and Xu, Q. Multi-patch prediction: Adapting llms for time series representation learning. *International Conference on Machine Learning*, 2024.

Cao, Z., Deng, J., Yu, L., Zhou, W., Liu, Z., Ding, B., and Zhao, H. Remember me, refine me: A dynamic procedural memory framework for experience-driven agent evolution. *arXiv preprint arXiv:2512.10696*, 2025.

Cheng, M., Liu, Z., Tao, X., Liu, Q., Zhang, J., Pan, T., Zhang, S., He, P., Zhang, X., Wang, D., et al. A comprehensive survey of time series forecasting: Concepts, challenges, and future directions. *Authorea Preprints*, 2025a.

Cheng, M., Wang, J., Wang, D., Tao, X., Liu, Q., and Chen, E. Can slow-thinking llms reason over time? empirical studies in time series forecasting. *arXiv preprint arXiv:2505.24511*, 2025b.

Cheng, M., Yang, J., Pan, T., Liu, Q., Li, Z., and Wang, S. Convtimeenet: A deep hierarchical fully convolutional model for multivariate time series analysis. In *Companion Proceedings of the ACM on Web Conference 2025*, pp. 171–180, 2025c.

Chow, W., Gardiner, L., Hallgrímsson, H. T., Xu, M. A., and Ren, S. Y. Towards time series reasoning with llms. *arXiv preprint arXiv:2409.11376*, 2024.

Feng, F., He, X., Wang, X., Luo, C., Liu, Y., and Chua, T.-S. Temporal relational ranking for stock prediction. *ACM Transactions on Information Systems (TOIS)*, 37(2):1–30, 2019.

Gruver, N., Finzi, M., Qiu, S., and Wilson, A. G. Large language models are zero-shot time series forecasters. *Advances in Neural Information Processing Systems*, 36: 19622–19635, 2023.

Huang, Q., Zhou, Z., Yang, K., and Wang, Y. Exploiting language power for time series forecasting with exogenous variables. In *Proceedings of the ACM on Web Conference 2025*, pp. 4043–4052, 2025a.

Huang, Q., Zhou, Z., Yang, K., Yi, Z., Wang, X., and Wang, Y. Timebase: The power of minimalism in efficient long-term time series forecasting. In *Forty-second International Conference on Machine Learning*, 2025b.

Hyndman, R. J. and Khandakar, Y. Automatic time series forecasting: the forecast package for r. *Journal of statistical software*, 27:1–22, 2008.

iFLYTEK AI Challenge. 2025 iflytek renewable power forecasting challenge (wind & solar). <https://challenge.xfyun.cn/topic/info?type=renewable-power-forecast&option=ssgy&ch=dwsf259>, 2025. Accessed: 2026-01.

Jia, F., Wang, K., Zheng, Y., Cao, D., and Liu, Y. Gpt4mts: Prompt-based large language model for multimodal time-series forecasting. In *Proceedings of the AAAI Conference on Artificial Intelligence*, volume 38, pp. 23343–23351, 2024.

Jiang, Y., Yu, W., Lee, G., Song, D., Shin, K., Cheng, W., Liu, Y., and Chen, H. Timexl: Explainable multi-modal time series prediction with llm-in-the-loop. In *The Thirty-ninth Annual Conference on Neural Information Processing Systems*, 2025.

Jin, M., Wang, S., Ma, L., Chu, Z., Zhang, J. Y., Shi, X., Chen, P.-Y., Liang, Y., Li, Y.-F., Pan, S., et al. Timeilm: Time series forecasting by reprogramming large language models. In *The Twelfth International Conference on Learning Representations*, 2024.

Lago, J., Marcjasz, G., De Schutter, B., and Weron, R. Forecasting day-ahead electricity prices: A review of state-of-the-art algorithms, best practices and an open-access benchmark. *Applied Energy*, 293:116983, 2021.

Lin, S., Chen, H., Wu, H., Qiu, C., and Lin, W. Temporal query network for efficient multivariate time series forecasting. In *Forty-second International Conference on Machine Learning*, 2025.

Liu, C., Xu, Q., Miao, H., Yang, S., Zhang, L., Long, C., Li, Z., and Zhao, R. Timecma: Towards llm-empowered multivariate time series forecasting via cross-modality alignment. In *Proceedings of the AAAI Conference on Artificial Intelligence*, volume 39, pp. 18780–18788, 2025a.

Liu, H., Zhao, Z., Wang, J., Kamarthi, H., and Prakash, B. A. Lstprompt: Large language models as zero-shot time series forecasters by long-short-term prompting. *arXiv preprint arXiv:2402.16132*, 2024a.

Liu, P., Guo, H., Dai, T., Li, N., Bao, J., Ren, X., Jiang, Y., and Xia, S.-T. Calf: Aligning llms for time series forecasting via cross-modal fine-tuning. In *Proceedings of the AAAI Conference on Artificial Intelligence*, volume 39, pp. 18915–18923, 2025b.

Liu, Y., Wu, H., Wang, J., and Long, M. Non-stationary transformers: Exploring the stationarity in time series forecasting. *Advances in neural information processing systems*, 35:9881–9893, 2022.

Liu, Y., Hu, T., Zhang, H., Wu, H., Wang, S., Ma, L., and Long, M. itransformer: Inverted transformers are effective for time series forecasting. In *The Twelfth International Conference on Learning Representations*, 2024b.

Luo, Y., Zhou, Y., Cheng, M., Wang, J., Wang, D., Pan, T., and Zhang, J. Time series forecasting as reasoning: A slow-thinking approach with reinforced llms. *arXiv preprint arXiv:2506.10630*, 2025.

Makovoz, D. and Marleau, F. R. Point-source extraction with mopex. *Publications of the Astronomical Society of the Pacific*, 117(836):1113, 2005.

Nie, Y., H. Nguyen, N., Sinthong, P., and Kalagnanam, J. A time series is worth 64 words: Long-term forecasting with transformers. In *International Conference on Learning Representations*, 2023.

Pan, Z., Jiang, Y., Garg, S., Schneider, A., Nevyvaka, Y., and Song, D. S²ip-llm: Semantic space informed prompt learning with llm for time series forecasting. In *Forty-first International Conference on Machine Learning*, 2024.

Qiu, X., Hu, J., Zhou, L., Wu, X., Du, J., Zhang, B., Guo, C., Zhou, A., Jensen, C. S., Sheng, Z., et al. Tfb: Towards comprehensive and fair benchmarking of time series forecasting methods. *arXiv preprint arXiv:2403.20150*, 2024.

Shi, F., Yin, X., Wang, K., Tu, W., Sun, Q., and Ning, H. Large language models for time series analysis: Techniques, applications, and challenges. *arXiv preprint arXiv:2506.11040*, 2025a.

Shi, X., Wang, S., Nie, Y., Li, D., Ye, Z., Wen, Q., and Jin, M. Time-moe: Billion-scale time series foundation models with mixture of experts. In *The Thirteenth International Conference on Learning Representations*, 2025b.

Singh, A., Fry, A., Perelman, A., Tart, A., Ganesh, A., El-Kishky, A., McLaughlin, A., Low, A., Ostrow, A., Ananthram, A., et al. Openai gpt-5 system card. *arXiv preprint arXiv:2601.03267*, 2025.

Tang, H., Zhang, C., Jin, M., Yu, Q., Wang, Z., Jin, X., Zhang, Y., and Du, M. Time series forecasting with llms: Understanding and enhancing model capabilities. *ACM SIGKDD Explorations Newsletter*, 26(2):109–118, 2025.

Taylor, S. J. and Letham, B. Forecasting at scale. *The American Statistician*, 72(1):37–45, 2018.

Tire, K., Taga, E. O., Ildiz, M. E., and Oymak, S. Retrieval augmented time series forecasting. *arXiv preprint arXiv:2411.08249*, 2024.

Wang, D., Cheng, M., Liu, Z., and Liu, Q. Timedart: A diffusion autoregressive transformer for self-supervised time series representation, 2025.

Wang, Y., Smola, A., Maddix, D., Gasthaus, J., Foster, D., and Januschowski, T. Deep factors for forecasting. In *International conference on machine learning*, pp. 6607–6617. PMLR, 2019.

Wang, Y., Wu, H., Dong, J., Qin, G., Zhang, H., Liu, Y., Qiu, Y., Wang, J., and Long, M. Timexer: Empowering transformers for time series forecasting with exogenous variables. *Advances in Neural Information Processing Systems*, 37:469–498, 2024.

Winters, P. R. Forecasting sales by exponentially weighted moving averages. *Management science*, 6(3):324–342, 1960.

Xue, H. and Salim, F. D. Promptcast: A new prompt-based learning paradigm for time series forecasting. *IEEE Transactions on Knowledge and Data Engineering*, 36(11):6851–6864, 2023.

Yang, S., Wang, D., Zheng, H., and Jin, R. Timerag: Boosting llm time series forecasting via retrieval-augmented generation. In *ICASSP 2025-2025 IEEE International Conference on Acoustics, Speech and Signal Processing (ICASSP)*, pp. 1–5. IEEE, 2025.

Zeng, A., Chen, M., Zhang, L., and Xu, Q. Are transformers effective for time series forecasting? In *Proceedings of the AAAI conference on artificial intelligence*, volume 37, pp. 11121–11128, 2023.

Zhang, W., Yin, C., Liu, H., Zhou, X., and Xiong, H. Irregular multivariate time series forecasting: A transformable patching graph neural networks approach. In *Forty-first International Conference on Machine Learning*, 2024.

Zhao, W. X., Zhou, K., Li, J., Tang, T., Wang, X., Hou, Y., Min, Y., Zhang, B., Zhang, J., Dong, Z., et al. A survey of large language models. *arXiv preprint arXiv:2303.18223*, 1(2), 2023.

Zhou, H., Zhang, S., Peng, J., Zhang, S., Li, J., Xiong, H., and Zhang, W. Informer: Beyond efficient transformer for long sequence time-series forecasting. In *Proceedings of the AAAI conference on artificial intelligence*, volume 35, pp. 11106–11115, 2021.

A. Appendix

A.1. Dataset Descriptions

Table 7. Dataset descriptions. The dataset size is organized in (Train, Validation, Test).

Dataset	Exogenous Descriptions	Endogenous Descriptions	Sampling Frequency	Dataset Size
NP	Grid Load, Wind Power	Nord Pool Electricity Price	1 Hour	(10224,1584,3024)
PJM	System Load, SyZonal COMED load	Pennsylvania-New Jersey-Maryland Electricity Price	1 Hour	(10224,1584,3024)
BE	Generation, System Load	Belgium's Electricity Price	1 Hour	(10224,1584,3024)
FR	Generation, System Load	France's Electricity Price	1 Hour	(10224,1584,3024)
DE	Wind power, Amprion zonal load	German's Electricity Price	1 Hour	(10224,1584,3024)
ETTh1	Power Load Feature	Oil Temperature	1 Hour	(8544,1344,2544)
ETTm1	Power Load Feature	Oil Temperature	15 Minutes	(16896,2496,4896)
WP	Meteorological Variables	Power Generation	15 Minutes	(16896,2496,4896)
SP	Meteorological Variables	Power Generation	15 Minutes	(16896,2496,4896)
MOPEX	Meteorological Forcing Variables	Daily Streamflow Discharge	1 Day	(8544,1344,2544)

We conduct a comprehensive evaluation of our method across diverse domains, covering both short-term and long-term forecasting tasks. The benchmarks include electricity prices, power load, renewable energy generation, and hydrological factors, featuring varying sampling frequencies from 15 minutes to 24 hours. See Table 7 for the detailed statistics.

Short-term Forecasting Benchmarks. We utilize five standard datasets from the Electricity Price Forecasting (EPF) benchmark¹, all sampled at an hourly frequency. These datasets are multivariate, containing past electricity prices along with distinct exogenous variables (e.g., load and generation forecasts) relevant to their respective markets:

- **Nord Pool (NP):** Sourced from the Nordic electricity market. It includes hourly electricity prices alongside exogenous forecasts for grid load and wind power generation.
- **Pennsylvania-New Jersey-Maryland (PJM):** Represents the US PJM interconnection. It features zonal electricity prices for the Commonwealth Edison (COMED) zone, incorporating system-wide load and zonal load forecasts as covariates.
- **Belgium (BE):** Sourced from the Belgian power exchange. It comprises hourly prices, domestic load forecasts, and cross-border generation forecasts from the French grid.
- **France (FR):** Represents the French electricity market. The dataset pairs hourly prices with corresponding national load forecasts and power generation predictions.
- **Germany (DE):** Sourced from the German market. It includes hourly prices, zonal load forecasts for the Amprion TSO area, and renewable energy forecasts for both wind and solar power generation.

Long-term Forecasting Benchmarks. For long-term horizons, we evaluate performance on datasets spanning industrial power transformers, renewable energy telemetry, and hydrological systems:

- **Electricity Transformer Temperature (ETTh1 & ETTm1):** A widely used benchmark for long-term forecasting². These datasets record the Oil Temperature (OT) and six load-type features from electricity transformers. **ETTh1** is sampled at an hourly frequency, while **ETTm1** is sampled every 15 minutes.
- **Wind Power (WP):** Derived from the iFLYTEK AI Developer Competition³, this dataset records the actual power output from a wind farm at a 15-minute resolution. It incorporates six meteorological covariates: direct radiation, wind speed (80m), wind direction (80m), temperature (2m), humidity (2m), and precipitation.
- **Sunny Power (SP):** Also sourced from the iFLYTEK competition with a 15-minute frequency. It tracks power generation from a separate renewable site and shares the same set of six meteorological features as the WP dataset.

¹<https://github.com/jeslago/epftoolbox>

²<https://github.com/zhouhaoyi/ETDataset>

³<https://challenge.xfun.cn/topic/info?type=renewable-power-forecast&option=ssgy&ch=dwsf259>

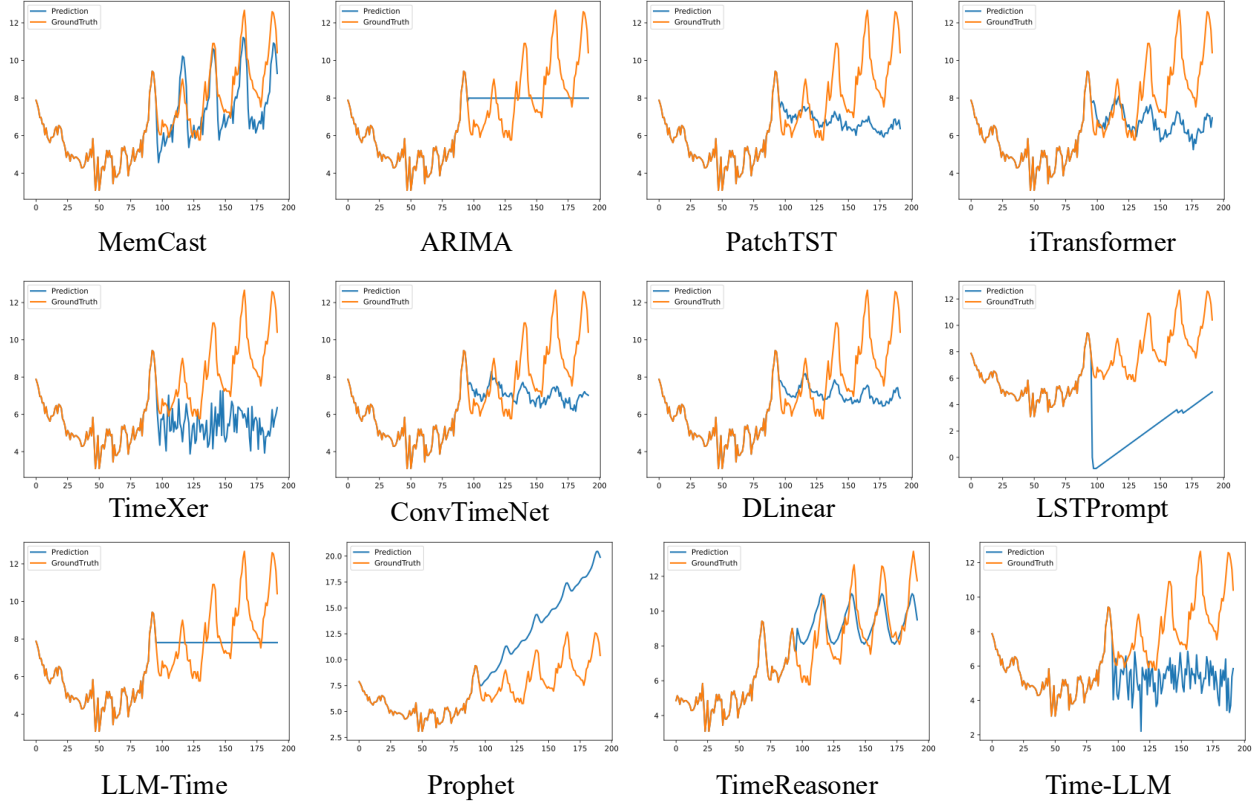


Figure 7. Qualitative visualization demonstrates that our framework captures complex non-stationary patterns and sharp fluctuations more accurately than state-of-the-art baselines, which generally suffer from significant lag or amplitude mismatch.

- **Model Parameter Estimation Experiment (MOPEX):** A hydrological dataset widely used for rainfall-runoff modeling⁴. Sampled at a daily frequency, it targets streamflow discharge prediction and includes four meteorological drivers: Mean Areal Precipitation (MAP), Climatic Potential Evaporation (CPE), Daily Maximum Air Temperature (T_{max}), and Daily Minimum Air Temperature (T_{min}).

A.2. Compared Baselines

We compare MemCast against a diverse set of representative baselines, ranging from classical statistical methods to state-of-the-art foundation models.

- **ARIMA** (Hyndman & Khandakar, 2008): A classic statistical method that models temporal patterns using autoregression, differencing, and moving averages to capture linear dependencies.
- **Prophet** (Taylor & Letham, 2018): An additive regression model designed for business time series, which effectively decomposes data into trends, seasonality, and holiday effects.
- **DLinear** (Zeng et al., 2023): A simple yet effective MLP-based model that utilizes a decomposition layer to handle trend and seasonal components separately.
- **PatchTST** (Nie et al., 2023): A Transformer-based model that introduces channel independence and patch-based tokenization to capture local semantic information and reduce computational complexity.
- **iTransformer** (Liu et al., 2024b): An inverted Transformer architecture that embeds the whole time series of each variate as a token and applies attention mechanisms across multivariate channels.

⁴<https://irsa.ipac.caltech.edu/data/SPITZER/docs/dataanalysistools/tools/mopex/>

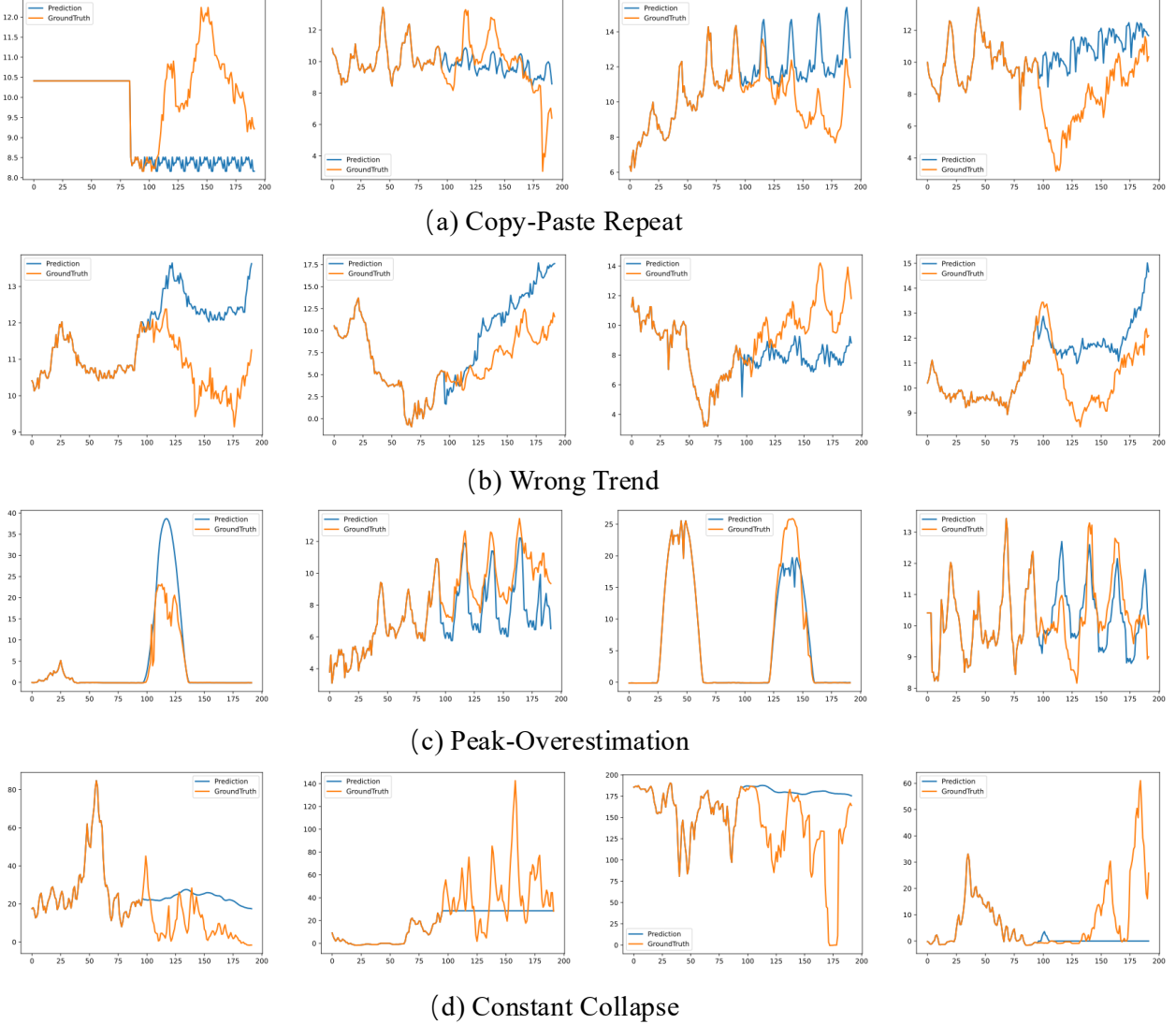


Figure 8. Visualization of typical failure modes: (a) Copy-Paste Repeat (naive history replication); (b) Wrong Trend (significant trajectory divergence); (c) Peak-Overestimation (amplitude exaggeration); and (d) Constant Collapse (degeneration into uninformative flat lines).

- **TimeXer** (Wang et al., 2024): An advanced Transformer framework designed to effectively empower time series forecasting by incorporating and aligning exogenous variables.
- **ConvTimeNet** (Cheng et al., 2025c): A deep hierarchical fully convolutional network that captures multi-scale temporal patterns through adaptive segmentation and deformable patching.
- **LSTPPrompt** (Liu et al., 2024a): An LLM-based method that decomposes time series into trend and seasonal components to construct specific prompts for guiding the language model’s forecasting.
- **LLM-Time** (Gruver et al., 2023): A zero-shot method that treats time series forecasting as a next-token prediction task by directly tokenizing numerical data for pre-trained LLMs.
- **TimeReasoner**: An approach that leverages the reasoning capabilities of LLMs to infer temporal dynamics and causal relationships within the time series data.
- **Time-LLM** (Jin et al., 2024): A comprehensive framework that aligns time series modalities with the text space of LLMs using reprogramming techniques and prompt-as-prefix strategies.

A.3. Visualization

Qualitative Analysis. To intuitively evaluate the forecasting capability of our framework, we visualize the prediction results of MemCast alongside state-of-the-art baselines on a representative challenging case characterized by high non-stationarity and sharp fluctuations, as shown in Figure 7.

Observations indicate distinct performance gaps across different model families. Traditional methods exhibit severe limitations: ARIMA degenerates into a flat line, failing to model any temporal dynamics, while Prophet captures a completely incorrect linear trend that diverges significantly from the ground truth. Deep learning baselines (e.g., PatchTST, DLinear, iTransformer), generally suffer from the "over-smoothing" problem; while they capture the general trend, they consistently underestimate the magnitude of sharp peaks and valleys and exhibit noticeable temporal lag. Other LLM-based approaches reveal stability issues; for instance, Time-LLM introduces significant high-frequency noise, and LSTPPrompt exhibits abrupt discontinuities and hallucinations.

In contrast, MemCast demonstrates superior robustness and precision. It successfully captures the evolving trend without the lag often seen in deep models and accurately reconstructs the amplitude of extreme fluctuations. This qualitative superiority validates that our memory-augmented reasoning mechanism effectively empowers the LLM to understand complex temporal patterns beyond simple pattern matching.

Failure Case Analysis. To provide a balanced and comprehensive evaluation, we visualize representative failure cases of MemCast in Figure 5, specifically focusing on the Oil Temperature forecasting task under out-of-distribution (OOD) covariates. While MemCast achieves superior performance on average, a detailed qualitative inspection reveals that it is not immune to reasoning errors when confronted with extreme distribution shifts or conflicting signals. We identify four distinct failure modes.

First, we observe **Copy-Paste Inertia**, where the model exhibits an over-reliance on retrieved memory, mechanically repeating historical patterns while ignoring immediate deviations in the input window. This suggests that strong retrieval relevance can occasionally suppress the model's adaptive reasoning. Second, the model may suffer from **Directional Misalignment**, where the forecasted trajectory diverges inversely from the ground truth. This is likely attributed to conflicting signals between the retrieved context and noisy covariates, leading the LLM to hallucinate an incorrect directional shift at critical turning points. Third, regarding **Amplitude Hypersensitivity**, the model correctly identifies the timing of events (e.g., spikes) but drastically exaggerates their magnitude. This implies that while the semantic reasoning captures the occurrence of fluctuations, the precise numerical scaling requires further calibration. Finally, **Degenerate Collapse** represents a failure where the generation degrades into a flat line, occurring when high uncertainty triggers excessive smoothing or when the LLM fails to construct a coherent temporal narrative.

These qualitative results highlight that explicitly grounding reasoning in historical experience, while effective, still faces challenges in OOD settings. The observed failures indicate that future work should focus on enhancing the conflict resolution mechanism between memory and current context, as well as improving the physical plausibility constraints to mitigate such hallucinations.

A.4. Detailed Prompt Construction

To effectively adapt the general reasoning capabilities of Large Language Models (LLMs) to the specialized task of time series forecasting, we design a comprehensive and structured prompting strategy. As illustrated in StrategyBox 1, our prompt is not merely a static input query but a dynamic, modular instruction set that bridges the modality gap between numerical time series data and textual logical reasoning. The prompt construction consists of four critical components, each serving a distinct role in guiding the model's generation process:

Role Initialization and Task Definition. The prompt begins by establishing a specialized persona ("expert time series forecaster") to activate the domain-specific latent knowledge of the LLM. It explicitly defines the forecasting horizon (e.g., $y_{t+1:t+24}$) and the available information scope, ensuring the model understands the input-output relationship and the boundaries of the task.

Experience-Conditioned Memory Retrieval. A core innovation of our framework is the injection of In-Context Memory. Unlike standard few-shot prompting that only provides positive examples, our retrieval module explicitly incorporates "Failure Modes" (e.g., Covariate-Miscalibration) and derived "Preventative Rules." By exposing the model to past mistakes

Forecasting Prompt

Role & Context: You are an expert time series forecaster. The task is to predict Nord Pool electricity prices ($y_{t+1:t+24}$) given a 168-hour history (\mathcal{H}) and 24-hour future covariate forecasts (\mathcal{F}).

In-Context Memory (Few-Shot Retrieval): You are provided with retrieved historical examples containing distinct failure modes. *Example excerpt: “Case 2 (Bad): [Covariate-Miscalibration]* The model applied fixed linear coefficients without validating against historical sensitivity, causing a +4.32 error.

Preventative Rule: Never apply absolute linear adjustments when deviations exceed 15% of the historical range.” Use these distilled lessons to avoid repeating documented errors.

Input Context Stream: The prompt structures the input into four blocks:

- (1) **Historical Data:** A serialized sequence of timestamps, Target OT , and covariates (Grid Load, Wind Power);
- (2) **Future Covariates:** Known future values for Load and Wind to guide the forecast trend;
- (3) **Statistical Summary:** Computed meta-features including μ , σ , trend slope, and lag-1 correlation (0.93);
- (4) **Visual Reasoning:** An automated analysis describing the current regime as “Oscillating trend with high volatility and pronounced intraday swings.”

Feedback & Constraints (Reflective Loop): The previous attempt triggered a strict Quality Control (QC) error: *Boundary jump too large* ($|\hat{y}_{t+1} - y_t| = 4.74 > 2.06$). You are now under **Hard Constraints:** The forecast must strictly maintain continuity with the last observed value ($y_t = 50.53$) and strictly bounded within [36.12, 65.29].

Instruction: Synthesize the retrieved lessons and visual insights, prioritize autoregressive patterns over covariate signals if the regime is stable. Generate the final vector $\hat{Y} \in \mathbb{R}^{24}$ in the strict format `<answer>...</answer>`.

(e.g., applying absolute linear coefficients without validation), we enforce a “negative constraint” mechanism, effectively instructing the model on what not to do, thereby reducing hallucination and improving logical robustness.

Multi-View Context Integration. To enable holistic reasoning, the context aggregates data from multiple views:

- Serialized Data: Converts the raw numerical history and future covariates into a sequence accessible to the LLM.
- Statistical Summary: Provides computed meta-features (e.g., mean μ , standard deviation σ , trend slope) to anchor the model’s numerical sensitivity.
- Visual Reasoning: Includes a textual description of the series’ morphological characteristics (e.g., “Oscillating trend,” “Intraday swings”). This translates visual patterns into semantic descriptions, aiding the LLM in identifying regime shifts that are difficult to discern from raw numbers alone.

Dynamic Feedback and Constraint Injection. The final component represents the “Reflective Loop” of our framework. If a previous forecast violates physical constraints or fails Quality Control (QC) checks (e.g., a “Boundary jump too large”), the system dynamically appends specific error feedback and hard constraints (e.g., strict boundary ranges [36.12, 65.29]) to the prompt. This transforms the forecasting process from a one-shot generation into an iterative refinement, ensuring that the final output maintains physical plausibility and continuity.